Receptor-mediated Endocytosis of Transferrin and Recycling of the Transferrin Receptor in Rat Reticulocytes

CLIFFORD HARDING, JOHN HEUSER, and PHILIP STAHL
Department of Physiology and Biophysics, Washington University School of Medicine, St. Louis, Missouri 63110

ABSTRACT At 4°C transferrin bound to receptors on the reticulocyte plasma membrane, and at 37°C receptor-mediated endocytosis of transferrin occurred. Uptake at 37°C exceeded binding at 4°C by 2.5-fold and saturated after 20–30 min. During uptake at 37°C, bound transferrin was internalized into a trypsin-resistant space. Trypsinization at 4°C destroyed surface receptors, but with subsequent incubation at 37°C, surface receptors rapidly appeared (albeit in reduced numbers), and uptake occurred at a decreased level. After endocytosis, transferrin was released, apparently intact, into the extracellular space. At 37°C colloidal gold-transferrin (AuTf) clustered in coated pits and then appeared inside various intracellular membrane-bounded compartments. Small vesicles and tubules were labeled after short (5–10 min) incubations at 37°C. Larger multivesicular endosomes became heavily labeled after longer (20–35 min) incubations. Multivesicular endosomes apparently fused with the plasma membrane and released their contents by exocytosis. None of these organelles appeared to be lysosomal in nature, and 98% of intracellular AuTf was localized in acid phosphatase-negative compartments. AuTf, like transferrin, was released with subsequent incubation at 37°C. Freeze-dried and freeze-fractured reticulocytes confirmed the distribution of AuTf in reticulocytes and revealed the presence of clathrin-coated patches amidst the spectrin coating the inner surface of the plasma membrane. These data suggest that transferrin is internalized via coated pits and vesicles and demonstrate that transferrin and its receptor are recycled back to the plasma membrane after endocytosis.

Receptor-mediated binding and endocytosis of transferrin occur in many cell types (4, 17, 23, 24, 34, 38) and appear to be requisite steps in iron delivery under some conditions (7, 9). Transferrin uptake has been best studied in erythropoietic cells, where the synthesis of hemoglobin requires a large amount of iron. Expression of transferrin receptors in these cells peaks early in development and declines progressively during the maturation of erythroblasts and reticulocytes (23, 34, 36). Despite their lower level of receptor expression, reticulocytes are a convenient model system, since they may be easily isolated from the blood of anemic animals.

Transferrin binding is mediated by protease-sensitive receptors (8) but is not inhibited by glycosidase treatment of either transferrin or its receptor (8, 18, 22). Transferrin receptors have been identified and characterized by many research groups. The uptake of transferrin is both temperature and energy dependent, and transferrin endocytosis has been demonstrated by the use of EM-autoradiography (9, 21), ferritin- or horseradish peroxidase-conjugated transferrin (9, 31), and ferritin-conjugated antitransferrin antibodies (31). These techniques reveal that transferrin binds to the plasma membrane at 4°C and appears inside intracellular vesicles during incubation at 37°C. Receptor-mediated transferrin uptake may occur by mechanisms similar to the uptake of other ligands: namely, clustering in coated pits and endocytosis via coated vesicles.

In this paper we present further biochemical data concerning transferrin endocytosis and provide evidence for the recycling of the transferrin receptor. Additionally, we report the use of various morphologic techniques to examine the mech-

THE JOURNAL OF CELL BIOLOGY · VOLUME 97 AUGUST 1983 329–339

anism of endocytosis in these cells, and we further define the intracellular compartments through which internalized transferrin passes.

MATERIALS AND METHODS

Ligand: Transferrin from pooled human serum (Calbiochem-Behring Corp., San Diego, CA or Sigma Chemical Co., St. Louis, MO) was tested for purity by SDS PAGE. Diferric transferrin was used in all experiments and was produced by the method of Galbraith et al. (5). Iodinations were performed by the chloramine T method as modified by Stahl et al. (30), except that 200 μg (20 μl) of chloroamine T was added to 200 μg of transferrin in a total volume of 130 μl. 15-nm colloidal gold beads were made by the citrate method (5 μg $HAuCl_4$ in 50 ml of boiling distilled H_2O plus 1.6 ml of 1% sodium citrate) and conjugated to transferrin at pH 5.7 (15, 29). Generally, 5 μg of transferrin was bound per milliliter of gold colloid; the resultant beads were used without polyethylene glycol stabilization. Colloidal gold-transferrin (AuTf)[1] was centrifuged at 10,000 *g* for 90 min, and the loose pellet of beads was resuspended in a small volume and dialyzed against mammalian Ringer's (155 mM NaCl, 5 mM KCl, 4 mM $CaCl_2$, 2 mM $MgCl_2$, 0.5 mM NaH_2PO_4, 10 mM glucose, 5 mM HEPES, pH 7.4).

Cells: Anemia was induced in 300–500-g male rats by administration of 1% aqueous phenylhydrazine i.p., typically 1.5 ml on days 0 and 1 and 1.0 ml on days 3 and 5. At least 2 d elapsed between the last phenylhydrazine administration and reticulocyte harvesting. Blood was harvested into heparinized (10 U/ml) Ca^{++}-free Ringer's (155 mM NaCl, 5 mM KCl, 6 mM $MgCl_2$, 4 mM EGTA, 0.5 mM NaH_2PO_4, 10 mM glucose, 5 mM HEPES, pH 7.4) by bleeding from the tail or by cardiac puncture using a heparinized syringe. Blood was centrifuged at 1,000 *g* for 5 min, the buffy coat was removed, and the cells were washed five times in Ringer's. Reticulocyte counts were generally about 90%.

Binding and Uptake Assays: Studies of binding at 4°C and uptake at 37°C were performed using the methods of Stahl et al. (30). 1–2 × 10^6 cells were used per tube, and incubations were performed in Ringer's. Bound ligand was separated from free ligand by spinning the cells through oil (30). Unless otherwise noted, saturating ligand concentrations were used (20 μg/ml at 5 × 10^5 cpm/μg for 20 min at 37°C, 6 μg/ml at 10^6 cpm/μg for 90 min at 4°C), and nonspecific binding was determined by the addition of excess unlabeled transferrin (1 mg/ml). Trypsinization was performed for 40 min at 4°C using 2 mg/ml trypsin (Sigma type III, Sigma Chemical Co.). For posttrypsinization binding or uptake studies, an equal volume of 2 mg/ml soybean trypsin inhibitor (Sigma type I-S Sigma Chemical Co.) was added, and the cells were centrifuged and resuspended in Ringer's. Dissociation of bound, iodinated ligand was measured in the presence of unlabeled transferrin in Ringer's (0.2 mg/ml and 1 mg/ml at 4° and 37°C, respectively). After spinning the cells through oil, 100 μl of each supernatant was precipitated by the addition of 100 μl of 10% BSA and 500 μl of 5% phosphotungstic acid in 2 N HCl. The samples were centrifuged in a Beckman microfuge (Beckman Instruments, Palo Alto, CA), and the ^{125}I contained in the pellets and supernatants was determined.

Preparations of Samples for Electron Microscopy: For AuTf uptake, 0.1 ml of packed reticulocytes was incubated in 0.5 ml of Ringer's with AuTf derived from 4 ml of the original colloid by centrifugation. Uptake of beads was blocked by the addition of 2 mg/ml excess unconjugated transferrin. After incubation with AuTf, 14.5 ml of Ringer's at 4°C was added and the cells were centrifuged, washed once in 15 ml of Ringer's at 4°C, and resuspended in 15 ml of $fixative_{ext}$ (115 mM NaCl, 5 mM $CaCl_2$, 30 mM HEPES, pH 7.4, 1% glutaraldehyde, 2% formaldehyde) for 30 min to 2 h at 4°C. Some samples were postfixed in 0.5% OsO_4 in $buffer_{ext}$ (115 mM NaCl, 5 mM $CaCl_2$, 30 mM HEPES, pH 7.4) for 30 min. Fixed cells were washed in $buffer_{ext}$, suspended as a thick slurry in $buffer_{ext}$ or 15% MeOH in distilled H_2O, and quick-frozen by the method described by Heuser (10, 12). Briefly, the samples were placed on a small cushion of glutaraldehyde-fixed lung and rapidly frozen against a pure copper block cooled to 4°K with liquid helium. Some cells were suspended in $buffer_{ext}$ and quick-frozen without prior fixation. Freeze substitution was performed as previously described (14). Fixed samples were prepared without freezing and stained for acid phosphatase (using cytidine monophosphate as substrate) (1) or for arylsulfatase B (using *p*-nitrocatechol sulfate) (2). For examination of surface-bound AuTf, fixed cells were adsorbed to small (5-mm square) polylysine-coated coverslips (slips were coated by incubation in 2 mg/ml polylysine in distilled H_2O for 45 min, followed by extensive washing in distilled H_2O), rinsed in 15% MeOH in distilled H_2O, and immediately quick-frozen. To examine the inside of the plasma membrane, reticulocytes were adsorbed to polylysine-coated coverslips, rinsed in Ca^{++}-free Ringer's, scraped open in KHMgE (70 mM KCl, 5 mM $MgCl_2$, 3 mM EGTA, 30 mM HEPES, pH 7.0) using a platinum wire, transferred to $fixative_{int}$ (115 mM KCl, 5 mM $MgCl_2$, 3 mM EGTA, 30 mM HEPES, pH 7.0, 1% glutaraldehyde and 2% paraformaldehyde), washed in $buffer_{int}$ (115 mM KCl, 5 mM $MgCl_2$, 3 mM EGTA, 30 mM HEPES, pH 7.0), and subsequently quick-frozen as above.

Freeze-Fracture and Electron Microscopy: Frozen samples were freeze-fractured in a Balzers 301 (Balzers, Hudson, NH) at −196°C, deep-etched for 4 min at −93°C, and rotary-replicated at an angle of 24° with platinum and carbon. Samples on coverslips were freeze-dried at −85°C until dry (this generally required ~20 min) and similarly replicated. Freeze-fracture replicas were cleaned in chromic acid or Purex bleach (12) (gold beads are removed by chromic acid treatment). Replicas of freeze-dried samples were removed from coverslips with hydrofluoric acid and then cleaned in Purex. For the preparation of thin sections, frozen samples were freeze-substituted, stained, and embedded as previously described (14). Samples that were fixed, stained, embedded, and thin sectioned without freezing gave similar results. Silver sections were cut on a Porter-Blum MT-2 ultramicrotome (Porter Instrument Co., Inc., Hatfield, PA) and stained for 20 min with 10% uranyl acetate in 50% MeOH, 50% distilled H_2O, and for 2–5 min in 0.4% lead citrate in 0.15 N NaOH.

Replicas and sections were examined in a JEOL 100 CX electron microscope at 100 kV. Stereo micrographs were taken at ± 10° tilt. For bead and organelle counts, cells were initially screened at 5,000 × magnification and rejected if they appeared damaged or abnormal. Gold beads were then counted and categorized at magnifications of 40,000–75,000 ×.

RESULTS

Biochemical Approaches to Transferrin Endocytosis

Reticulocytes were incubated in the presence of ^{125}I-transferrin plus or minus excess unlabeled transferrin. At 4°C transferrin binding was found to be specific, saturable, and reversible. Binding was found to be essentially complete within 60 min; thereafter, an incubation time of 90 min was routinely used. Saturation of binding occurred at ~6 μg/ml (7.5×10^{-8} M), and a K_d of 2.0×10^{-8} M was estimated from a Scatchard plot. Extrapolation indicated that ~ 4.9×10^4 receptors were expressed on the surface of these cells. Dissociation at 4°C in the presence of 150 μg/ml unlabeled transferrin was found to occur with a $t_{1/2}$ of 80 min.

At 37°C saturation of ligand uptake occurred within 25–35 min. After a 35-min uptake cells were incubated in the presence of unlabeled transferrin (2.0 mg/ml) at 37°C. Release of cell-bound ^{125}I-transferrin occurred with $t_{1/2}$ = 8 min. The radioactivity released into the medium during the second incubation was 90% phosphotungstic acid-precipitable. This indicated that ^{125}I-transferrin uptake at 37°C was reversible and that under these conditions virtually all of the bound ligand was released into the medium in an essentially intact form. At 37°C saturation of ^{125}I-transferrin uptake occurred at ~ 7 μg/ml (8.8×10^{-7} M). A Scatchard plot indicated a K_{uptake} of 5.1×10^{-9} M and 1.2×10^5 receptors/cell. Comparison with the previous Scatchard data showed that 4°C-binding labeled 40% of the total receptors labeled at 37°C, indicating that ~ 60% of the receptors were inacessible and may be intracellular. The requirement of an equilibrium state for Scatchard analysis appeared to be met by the fact that both uptake to a steady state and release of bound ligand were virtually complete within 20–30 min. The number of receptors expressed per cell varied considerably (generally 1–3 × 10^5/cell) between experiments, as would be expected with a receptor number dependent on developmental stage, but the 4°C binding level was generally 35–40% of the 37°C uptake in the same cell population. No specific transferrin binding or uptake was observed with mature erythrocytes.

To investigate the distribution of ligand after 37°C uptake, trypsinization at 4°C was employed to distinguish cell surface

[1] *Abbreviations used in this paper:* AuTf, colloidal gold-transferrin; MVE, multivesicular endosome.

ligand from intracellular ligand. Following 25 min of incubation at 37°C, ~ 20–40% of the bound ligand was found to be trypsin resistant, indicating that internalization had occurred. (Some variability between experiments may have been caused by a varying amount of loss of intracellular ligand due to cell lysis during the trypsinization.) While these results, similar to those of Octave et al. (24), indicate that a minimum of 20–40% of the ligand bound at 37°C was intracellular, the actual internal fraction probably exceeded this value. The trypsin-resistant fraction was found to increase with time during 37°C incubation until a plateau was reached after 25–35 min. Either internalization of receptor-ligand complexes ceased at this time, or, more likely, a steady-state equilibrium was achieved where internalization was balanced by externalization of ligand or receptor-ligand complexes.

To determine whether receptors could be externalized, cells were pretrypsinized at 4°C, washed, and then incubated with ^{125}I-transferrin at 37°C (Fig. 1). Trypsinization at 4°C destroyed at least 94% of the original surface receptor pool (Fig. 2). Nonetheless, the subsequent uptake occurred with a similar time course but saturated at ~ 40% of uptake by untrypsinized cells of the same population. This indicated that trypsin-resistant receptors, presumably intracellular, replaced destroyed surface receptors to mediate transferrin uptake. Furthermore, uptake after 4°C-trypsinization was not significantly affected by the presence of cycloheximide (50 μg/ml), indicating that this uptake was not dependent on the synthesis of new receptors.

The existence of distinct internal and surface receptor pools that communicate only above 4°C was further demonstrated. Cells were trypsinized at 4°C, washed to remove trypsin, incubated without transferrin at 37°C, and cooled to 4°C; binding of ^{125}I-transferrin was then measured at 4°C (Fig. 2). Again, 4°C trypsinization destroyed the original pool of surface receptors, but subsequent incubation at 37°C allowed recovery of surface receptors to ~ 45–70% of pretrypsinization levels. These results confirm the existence of a trypsin-resistant (internal) pool of receptors that can replenish surface receptors destroyed by trypsin.

Morphologic Approaches to Transferrin Endocytosis

A number of techniques were used to visualize the process of transferrin endocytosis. AuTf was used as a morphologic probe for the transferrin receptor and the pathway of transferrin endocytosis. The specificity of AuTf binding was demonstrated by two methods. First, ^{125}I-transferrin was conjugated to gold beads and its uptake was assayed as described above for unconjugated iodinated ligand. Fig. 3 demonstrates that uptake of ^{125}I-labeled AuTf was inhibited by excess unlabeled, unconjugated ligand, indicating specific uptake. The possibility that bead-bound ^{125}I-transferrin is first released from the beads into free solution and then taken up is unlikely since the supernatant from a second 90-min bead centrifugation (after resuspension to the original volume in Ringer's) produced only 1–2% as much ^{125}I-transferrin uptake as the bead fraction (Fig. 3). Specificity of AuTf uptake was also demonstrated morphologically by adding excess unconjugated transferrin (2 mg/ml) to incubations of AuTf with reticulocytes. This almost eliminated the binding of AuTf to cell surfaces and to intracellular sites (Fig. 6). The kinetics of AuTf uptake were similar to those of unconjugated ^{125}I-transferrin, and ^{125}I-AuTf was released from the cells at 37°C with a $t_{1/2}$ of 8.5–10.7 min (within the range observed for unconjugated ^{125}I-transferrin). After a 35-min uptake at 37°C

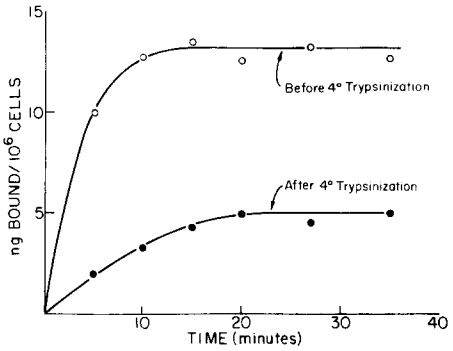

FIGURE 1 Uptake of ^{125}I-transferrin by rat reticulocytes after the destruction of surface receptors by 4°C trypsinization. Control reticulocytes were incubated with ^{125}I-transferrin (20 μg/ml) in Ringer's at 37°C for various periods. Other cells were trypsinized at 4°C, washed, and then incubated at 37°C as above. Specific uptakes of control cells (open circles) and pretrypsinized cells (solid circles) are shown as a function of incubation time.

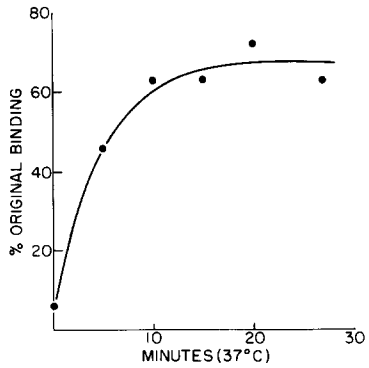

FIGURE 2 Recovery of 4°C binding during 37°C incubation following the destruction of surface receptors by 4°C trypsinization. Reticulocytes were trypsinized at 4°C, washed, incubated in Ringer's at 37°C for various periods, and cooled to 4°C. The cells were then incubated with ^{125}I-transferrin (6 μg/ml) for 90 min at 4°C. Specific binding is shown as a function of time of incubation at 37°C.

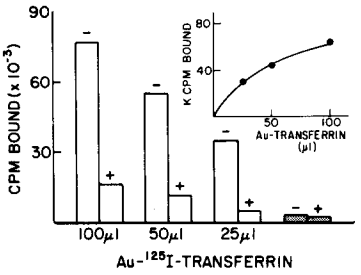

FIGURE 3 Specific uptake of ^{125}I-transferrin conjugated to colloidal gold by reticulocytes at 37°C. ^{125}I-transferrin-conjugated gold colloid was prepared, centrifuged, and suspended in Ringer's. Aliquots (100, 50, and 25 μl) of this suspension were incubated with reticulocytes for 30 min at 37°C in a final volume of 200 μl. The first three pairs of bars show uptake in the absence (−) and presence (+) of unlabeled, unconjugated transferrin (1 mg/ml final concentration). *Inset*: specific uptake as a function of the amount of colloid added to the cells. In addition, 100 μl of the supernatant from a second colloid centrifugation was similarly incubated with reticulocytes; the uptake observed in the absence (−) and presence (+) of unlabeled, unconjugated transferrin is indicated by the stippled bars on the right.

and a 35-min chase at 37°C with cold, unconjugated transferrin, the cells were removed by centrifugation (1,000 *g* for 5 min); 71% of the phosphotungstic acid-precipitable radioactivity remaining in the supernatant was pelleted by centrifugation at 20,000 *g* for 75 min. This suggests that most of the released ^{125}I-transferrin was still associated with gold beads and/or with membrane-bound vesicles released by multivesicular endosome (MVE) exocytosis (see below).

AuTf binding to the plasma membrane was demonstrated by incubating reticulocytes with AuTf at 37°C, washing with Ringer's at 4°C, and fixing with fixative$_{ext}$ at 4°C. Fixed cells were then adsorbed onto polylysine-coated coverslips, quick-frozen, freeze-dried, and rotary-replicated. The resulting replicas retained surface-bound gold beads, strikingly illustrating the distribution of transferrin receptors on the plasma membrane. AuTf was found scattered randomly on the cell surface and clustered in membrane pits (Figs. 4 and 5). To study the distribution of intracellular AuTf, incubations were similarly performed, but cells were quick-frozen in a thick suspension. Some cells were quick-frozen without prior fixation. These samples were then freeze-substituted, stained, and embedded for thin sectioning. Fig. 7 shows thin sections of reticulocytes incubated with AuTf for 5 min at 37°C. AuTf is localized to the free surface of the plasma membrane, within coated pits and vesicles (~ 100 nm o. d.), inside small uncoated vesicles of varying size (<200 nm; generally ~ 100 nm diam), and inside tubular structures (usually 60–80 nm diam) (Fig. 8). Some vesicular profiles may represent cross-sections of tubular compartments. The clathrin coat is sometimes difficult to discern in thin sections, since the reticulocyte cytoplasm stains so densely that it can mask the presence of a densely staining coat on the cytoplasmic surface of membrane structures.

When reticulocytes were incubated for 20 min or longer at 37°C, AuTf was also found within MVE (see Fig. 9). These structures are often 250–300 nm diam but range from 120 to 800 nm diam and may be irregularly shaped. Included in this class are membrane-bounded structures that contain distinct vesicular inclusions as well as others that contain more amorphous inclusions that stain with a density similar to that of the cytoplasm. In some cases vesicular inclusions may represent cytoplasmic protrusions into the lumen of the MVE; such protrusions were occasionally visualized. MVE were often heavily labeled, with one structure containing many gold beads. The beads frequently appeared to be associated with the membranes and inclusions of the MVE.

The enzyme content of MVE was explored to determine whether or not these structures contained lysosomal enzymes. Acid phosphatase staining was performed using cytidine monophosphate as the substrate (1). Figs. 10 and 11 demonstrate that this procedure stained reticulocyte lysosomes but did not stain MVE. Arylsulfatase staining also failed to stain MVE. Thus, MVE differ from some other multivesicular bodies, which often contain acid phosphatase and other lysosomal enzymes. In fact, 98% of intracellular AuTf was observed in acid phosphatase-negative compartments. Most lysosomal structures did not contain AuTf, but occasionally these structures did contain a small number of beads. These data indicated that transferrin processing occurred in nonlysosomal compartments.

Table I shows the time course of distribution of AuTf among various compartments. In our analysis, coated vesicles, small uncoated vesicles, and tubular structures represent one kinetic class; these structures all contained AuTf after 5 min of uptake at 37°C. (Differences in the rate of labeling between these compartments may exist but were not discernible by our methods.) MVE, on the other hand, were labeled only rarely in 5–10-min incubations, but by 35 min they contained 17% of the cell-bound AuTf. MVE were observed in reticulocytes after all periods of incubation at 37°C, and counts indicated that their abundance did not vary significantly between 5 and 35 min of incubation with AuTf at 37°C. Therefore, the increased percentage of beads residing in MVE was due to an increase in the density of MVE labeling rather than an increase in MVE number. For example, MVE in reticulocytes incubated with AuTf for 5–10 min at 37°C were sparsely labeled (0–3 beads/MVE), whereas the longer incubations produced much denser labeling (sometimes exceeding 70 beads in one MVE). Even after 35-min incubations, labeled MVE were much less common than other labeled compartments, but they contained a disproportionately large fraction of the beads owing to their heavy labeling.

To examine the recycling of AuTf, reticulocytes were incubated with AuTf for 35 min at 37°C, washed in 4°C Ringer's, and incubated in the presence of 2 mg/ml unconjugated transferrin for 25 min at 37°C. These cells were examined in thin sections, and cell-bound AuTf was quantitated to determine the fate of endocytosed AuTf. After 25 min of chase, the average number of beads bound per cell section decreased to 22% of the level found in control (unchased) samples, indicating that endocytosed AuTf was released from reticulocytes upon subsequent incubation. The cellular distribution of AuTf also changed (Table I). Beads were virtually nonexistent inside coated pits, presumably owing to competition by unconjugated transferrin, and the chase also decreased the frequency of AuTf-labeling of small vesicles and tubules. Although the absolute level (beads per organelle per cell section) of MVE labeling was also decreased, the fraction of cell-bound beads inside MVE rose to 38%. This indicated that MVE represent a late stage in transferrin processing in the reticulocyte.

An additional observation in this experiment was the apparent exocytosis of AuTf-labeled MVE with the consequent release of the vesicular inclusions into the extracellular space (Figs. 12–17). Often vesicles similar to those found in MVE were found attached to the plasma membrane (Figs. 15 and 17). Furthermore, 54% of the AuTf found on the free surface of the cells after the chase was associated with adherent vesicular inclusions, and another 21% occurred in clusters that looked as though they might have been the remains of a MVE exocytic event. These results suggested that at least some of the transferrin that accumulated inside MVE was eventually released by exocytosis.

The distribution of AuTf in reticulocytes described above has been confirmed by several techniques. After incubation with AuTf, reticulocytes were quick-frozen without prior fixation to control for fixation artifacts. The results were identical to those obtained with fixed cells, including the accumulation of AuTf within MVE and the apparent exocytosis of AuTf-labeled MVE. Freeze-fracture studies confirmed the intracellular distribution of AuTf determined in thin sections (Figs. 18 and 19). Intracellular AuTf was not visualized in this type of preparation unless the samples were OsO_4-fixed before freezing. Otherwise, the fracture plane followed the membrane of intracellular vesicles and did not expose their lumen. In OsO_4-fixed cells that were freeze-fractured and deep-etched,

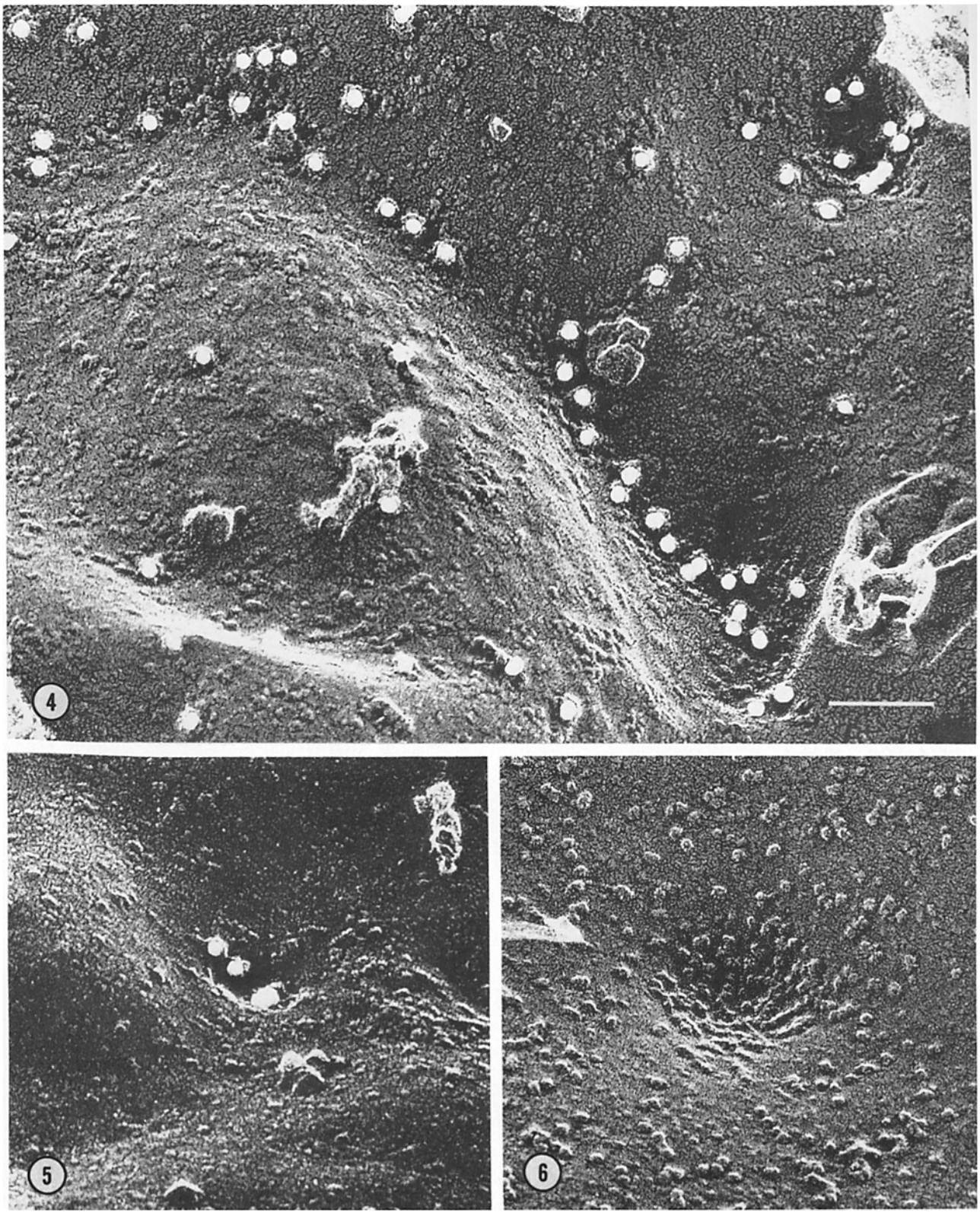

FIGURES 4–6 Fig. 4: View of the plasma membrane of a freeze-dried reticulocyte showing AuTf scattered on the membrane and clustered into a pit (*upper right*). Note that the reverse printing employed for pictures of platinum replicas makes the gold particles appear white. Bar, 100 nm. × 185,000. Fig. 5: AuTf clustered into a pit on the surface of a freeze-dried reticulocyte. × 185,000. Fig. 6: Typical view of a pit on the plasma membrane of a reticulocyte incubated with AuTf and 1 mg/ml unconjugated transferrin; virtually no AuTf binding remains in the presence of the competing ligand. × 185,000.

AuTf remained in the replicas, appearing within cross-fractured intracellular vesicles. This demonstrates that gold beads may be used in freeze-fracture studies to explore the distribution of both intracellular and extracellular ligands. Importantly, this provided a control for the differential loss of gold beads from organelles in thin sections. Fig. 19 shows an MVE

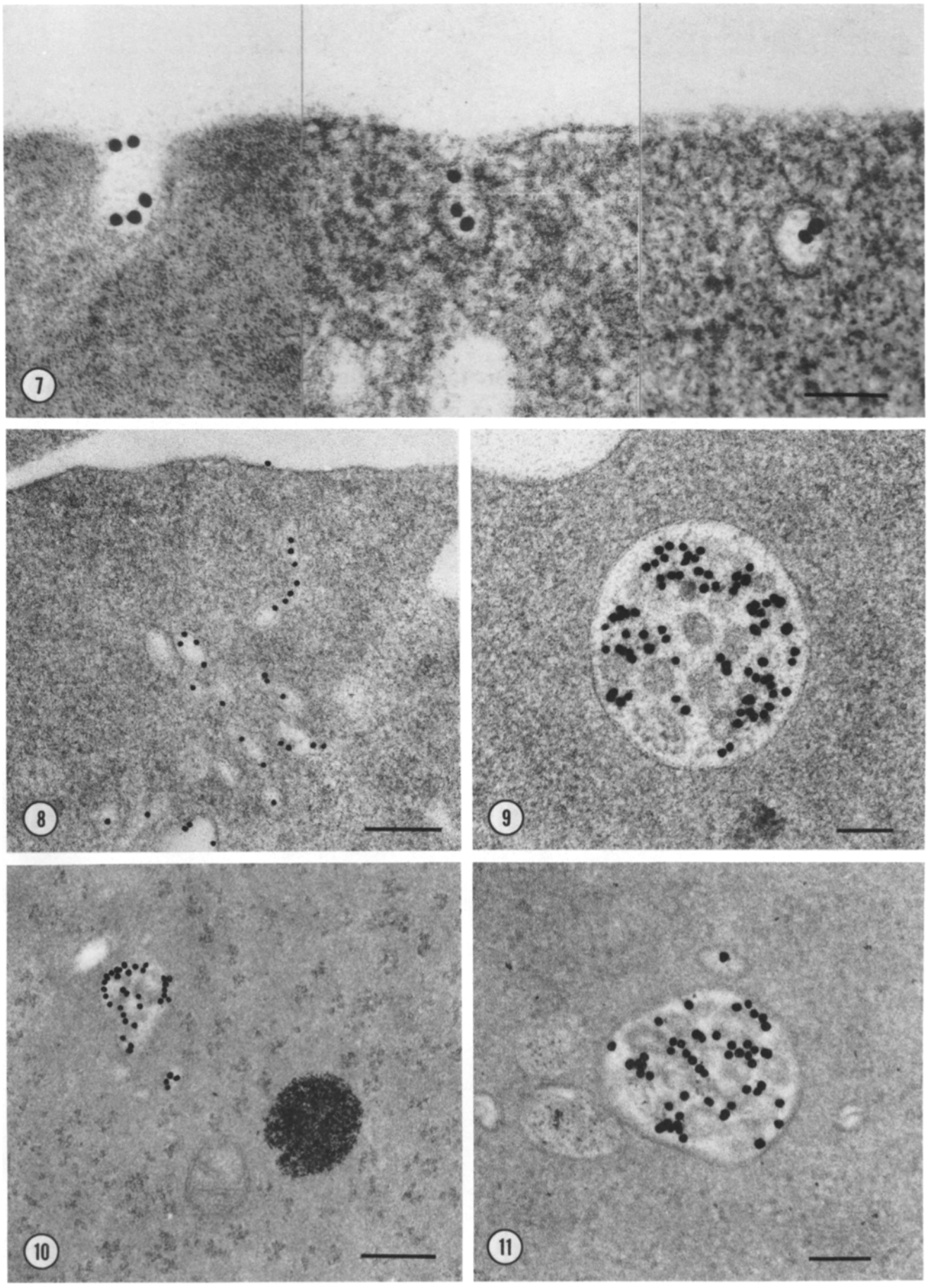

TABLE I

Distribution of AuTf in Reticulocytes after Incubation at 37°C

Duration of incubation	n	Plasma membrane free surface	Coated pits	Small vesicles and tubules	MVE	No. of beads per cell section
min			%			
5	305	26	15	58	1	3.0
10	312	27	11	59	3	5.1
20	318	17	9	61	13	8.5
35	345	24	11	48	17	12.0
35+ 25-chase	634	56*	0	6	38	2.4

* For the 25-min chase, cells were incubated with AuTf for 35 min, washed, and incubated with unconjugated transferrin (1 mg/ml) for 25 min. 56% of the beads were on the plasma membrane, but these were generally found in clusters and were often associated with adherent vesicles. These beads may largely represent the remnants of exocytotic events rather than association of AuTf from the medium with the plasma membrane.

with its vesicular inclusions which was labeled with AuTf during a 20-min incubation at 37°C. AuTf appears to be bound to the inner walls and vesicular inclusions of these vesicles. When viewed in stereo, intracellular vesicles appeared as bowl-like depressions in a mesa of etch-resistant cytoplasm; they etched more than the surrounding cytoplasm because they contained much less protein.

Due to the densely-staining nature of reticulocyte cytoplasm and other inherent limitations of the technique, thin sections do not provide good views of coated pit and vesicle formation in reticulocytes. More information concerning clathrin-coated structures can be obtained from platinum-carbon replicas (11). To further explore the morphologic basis of endocytosis, we used techniques developed earlier (10) to permeabilize or scrape open cells to remove the soluble cytoplasmic proteins. Following these treatments the samples were quick-frozen, freeze-fractured, deep-etched, and rotary-replicated. Triton extraction of reticulocytes largely removed the plasma membrane, leaving behind an erythrocyte-like cytoskeleton (devoid of microfilaments, microtubules, etc.). Clathrin-coated structures were observed within these samples. Saponin extraction left the plasma membrane more nearly intact but permeabilized the cell and released enough cytoplasmic proteins to reveal coated pits and vesicles. Soluble cytoplasmic proteins were also released by hypotonic lysis or were diluted by swelling the cells with hypotonic solutions; both treatments exposed coated pits on the plasma membrane. Finally, reticulocytes attached to polylysine-coated glass slips were scraped open, fixed, quick-frozen, and freeze-dried to reveal the proteins applied to the inner surface of the plasma membrane. Figs. 20 and 21 demonstrate the results of this approach, revealing coated structures surrounded by a background of fixed cytoskeletal proteins. Coated regions are usually 60–180 nm (mostly 80–140 nm) in diameter, slightly domed structures, viewed from this perspective. The size and conformation of coated pits may be restricted in this preparation, since the formation of coated pits may be altered by adherence to the cationic polylysine substrate. There is further variation in the size of clathrin patches, including very small clathrin aggregates. However, the large amounts of clathrin revealed by similar techniques in fibroblasts (11), hepatocytes (13), macrophages, lymphocytes, and bone marrow cells were not observed in reticulocytes. This may reflect a decreasing ability of maturing reticulocytes to perform receptor-mediated endocytosis.

DISCUSSION

The endocytosis of transferrin provides many interesting contrasts to other endocytotic systems, including those of the mammalian mannose and glactose receptors. Unlike these systems, transferrin binding is apparently not oligosaccharide mediated, since glycosidase treatment of transferrin or its receptor does not reduce transferrin binding (8, 18, 22). The mannose receptor of macrophages (30) and the galactose receptor of hepatocytes (16, 37, 41) both target their ligands largely to lysosomes, where they are degraded. These ligands dissociate from their receptors, probably in a prelysosomal acid compartment, allowing the receptors to separately recycle back to the cell surface (32, 33). Transferrin, however, is not degraded and is released intact from cells after endocytosis, indicating that it may largely avoid lysosomes during its intracellular passage. This is substantiated by our morphologic results, which indicated that 98% of intracellular AuTf resides in acid phosphatase-negative compartments. Furthermore, transferrin may remain largely associated with its receptor inside the cell. At 37°C ^{125}I-transferrin uptake saturated and appeared to satisfy the equilibrium requirments for Scatchard analysis, unlike ligands that dissociate from their receptors and accumulate within the cell. In some systems lysosomotropic amines interfere with receptor recycling and may inhibit receptor-ligand dissociation (32). In contrast, ^{125}I-transferrin uptake is relatively unaffected by these agents, while removal of the iron from transferrin is inhibited (20, 25, 26, 6a). Thus, intracellular transferrin-receptor complexes may enter a low pH environment, which is necessary for iron removal but does not affect the transferrin-receptor interaction (6a). The close association of AuTf with membrane surfaces in both thin-section and freeze-fracture studies also suggests a continued receptor-ligand interaction, although this association could be explained as nonspecific or as a fixation artifact. When reticulocytes were chased by exposure to free transferrin after incubation with AuTf, intracellular ligand was released. Small clusters of AuTf that remained attached to the cell surface after 35 min of chase may represent exocytosed receptor-ligand complexes. This suggests that, for transferrin, the receptor-ligand interaction remains intact

FIGURES 7–11 Fig. 7: Thin-section views of reticulocytes incubated with AuTf for 5 min at 37°C, showing AuTf clustering into coated pits and endocytosis via coated vesicles. Bar, 100 nm. × 155,000. Fig. 8: Small vesicles and tubules in the reticulocyte cytoplasm are labeled with AuTf after 5 min at 37°C. This figure shows these compartments more heavily labeled after a 20-min incubation. Bar, 200 nm. × 71,000. Fig. 9: View of an MVE in a reticulocyte that was incubated with AuTf for 30 min, quick-frozen without prior fixation, and freeze substituted. Bar, 100 nm. × 106,000. Figs. 10 and 11: Thin sections of reticulocytes stained for acid phosphatase. Lysosomes are heavily labeled, but MVE appear to be unlabeled. Fig. 10: bar, 200 nm. × 70,000. Fig. 11: bar, 100 nm. × 115,000.

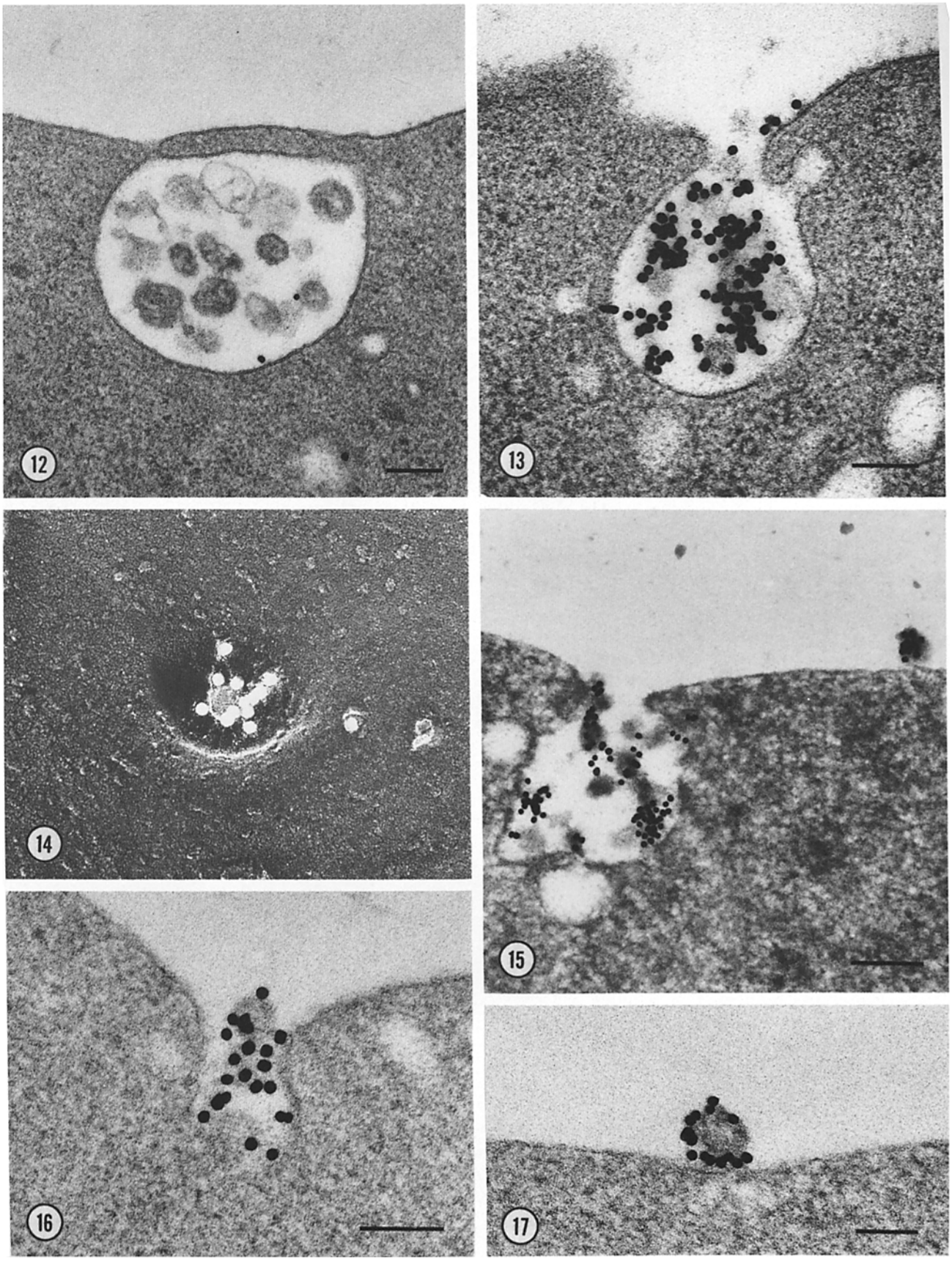

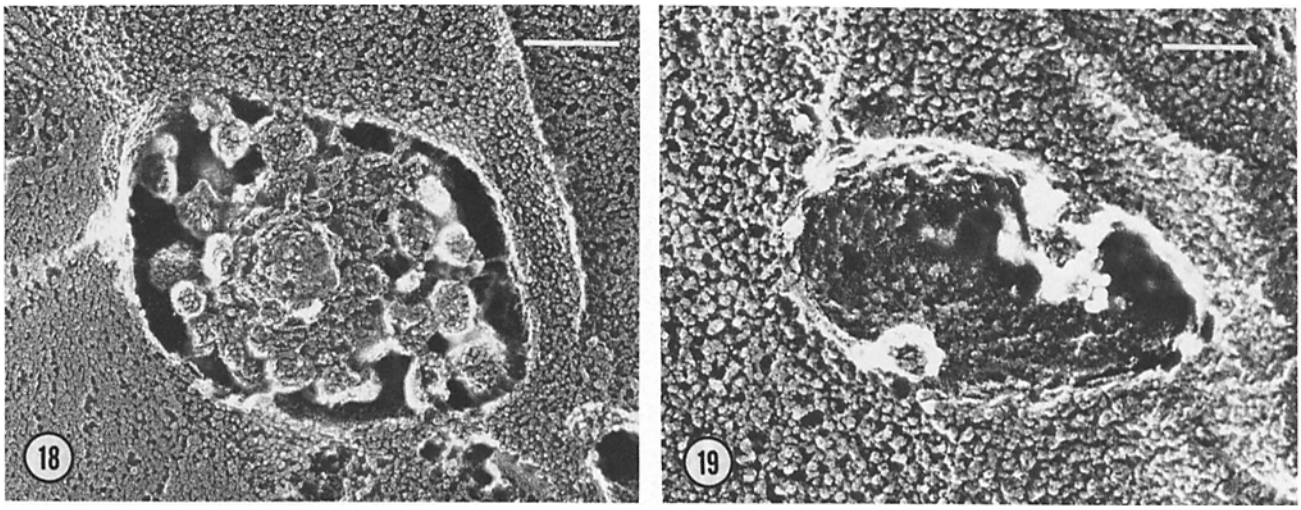

FIGURES 18 and 19 Fig. 18: Freeze-fracture, deep-etch view of a large MVE filled with numerous inclusions. The remaining free lumen possesses a markedly lower protein concentration than the surrounding cytoplasm and is deeply etched. Bar, 200 nm. × 63,000. Fig. 19: View of an MVE lightly labeled by AuTf after a 20-min incubation at 37°C. AuTf (white dots) is bound to the walls of the MVE and is clustered heavily around the inclusions, making the outline of the individual gold beads difficult to discern. Bar, 100 nm. × 127,000.

throughout endocytosis, leading to recycling of both receptor and ligand to the surface, in contrast to other receptor systems where receptor-ligand dissociation allows targeting of ligand to lysosomes and recycling of the unoccupied receptor. The fidelity of the transferrin-receptor interaction is fortunate, since this makes the ligand an unusually useful morphologic probe for its receptor.

The necessity of endocytosis for the removal of iron from transferrin continues to be questioned by some groups (6, 19, 27, 39, 40). Nonetheless, transferrin endocytosis has been well documented (9, 21, 31) and is confirmed by our results. Our morphologic data revealed that after 5–10 min of incubation at 37°C, most intracellular AuTf appeared inside small vesicular and tubular profiles. After 20–35 min of incubation, an increasing fraction appeared inside heavily labeled MVE. Transferrin-labeled structures of all types were mostly acid-phosphatase negative. MVE displayed a relatively slow time course of AuTf labeling, and these structures may represent a late stage in transferrin processing. If MVE represent an obligate step in transferrin/receptor recycling or iron removal, this would have important implications for the time course of the recycling process. Nunez et al. (23) calculated an iron uptake rate of 0.062 atom of iron/min/receptor for their orthochromatic erythroblast-reticulocyte fraction. This translates to one pair of iron atoms every 32 min for each receptor. Assuming removal of two iron atoms from each diferric transferrin internalized, this means that the average receptor cycle time is 32 min, which is kinetically compatible with passage of most receptor-ligand complexes through MVE. On the other hand, a shorter transferrin-receptor recycling time has been reported by other workers (35). This suggests that transferrin/receptor complexes may be recycled directly from the tubular and vesicular compartments without passing through MVE. Thus, MVE may be an optional detour rather than an obligate step in transferrin processing.

Recycling of transferrin-receptor complexes from MVE is supported by the apparent concomitant exocytosis of AuTf and vesicular inclusions derived from MVE. This may be observed in reticulocytes incubated with AuTf for 35 min at 37°C and after a subsequent 35-min chase with free transferrin. Exocytosis of vesicular inclusions could partially account for the loss of membrane surface area observed during reticulocyte maturation (3, 28). Zweig et al. (42) demonstrated that the cytoplasmic aspect of reticulocyte endosomes are free of spectrin by ferritin immunolabeling of ultrathin frozen sections, and they proposed that during reticulocyte maturation, these spectrin-free membranes are preferentially lost by intracellular degradation or by "exocytosis" (by which they mean inclusion in plasma membrane blebs that are removed in the spleen). We have demonstrated that MVE inclusions may be truly exocytosed (as opposed to the above process, which might be better termed "blebbing"), and this may provide an additional mechanism for the preferential loss of spectrin-free membrane. In some cases AuTf was associated

FIGURES 12–17 Fig. 12: View of an MVE sparsely labeled with AuTf after a 20-min incubation at 37°C. Note the apparent fusion of the MVE and the plasma membrane. This may represent incipient MVE exocytosis. Bar, 100 nm. × 107,000. Fig. 13: View of MVE exocytosis in an unfixed reticulocyte. This cell was incubated for 30 min with AuTf, subjected to a 20-min chase with unconjugated transferrin, and then quick-frozen without prior fixation and freeze-substituted. Bar, 200 nm. × 61,000. Fig. 14: Clustered AuTf and an associated vesicle in a membrane invagination on the surface of a freeze-dried reticulocyte, representing the exocytosis of a small MVE. × 156,000. Fig. 15: MVE exocytosis with concomitant release of vesicular inclusions. These vesicles often remain attached to the plasma membrane (*upper right*). Bar, 200 nm. × 68,000. Fig. 16: Exocytosis of a small AuTf-labeled MVE. Comparison with earlier figures reveals the variability in size of MVE and their exocytotic intermediates. Bar, 100 nm. × 156,000. Fig. 17: An adherent membrane vesicle with associated AuTf. This presumably represents the remnant of an MVE exocytosis. Bar, 100 nm. × 119,000.

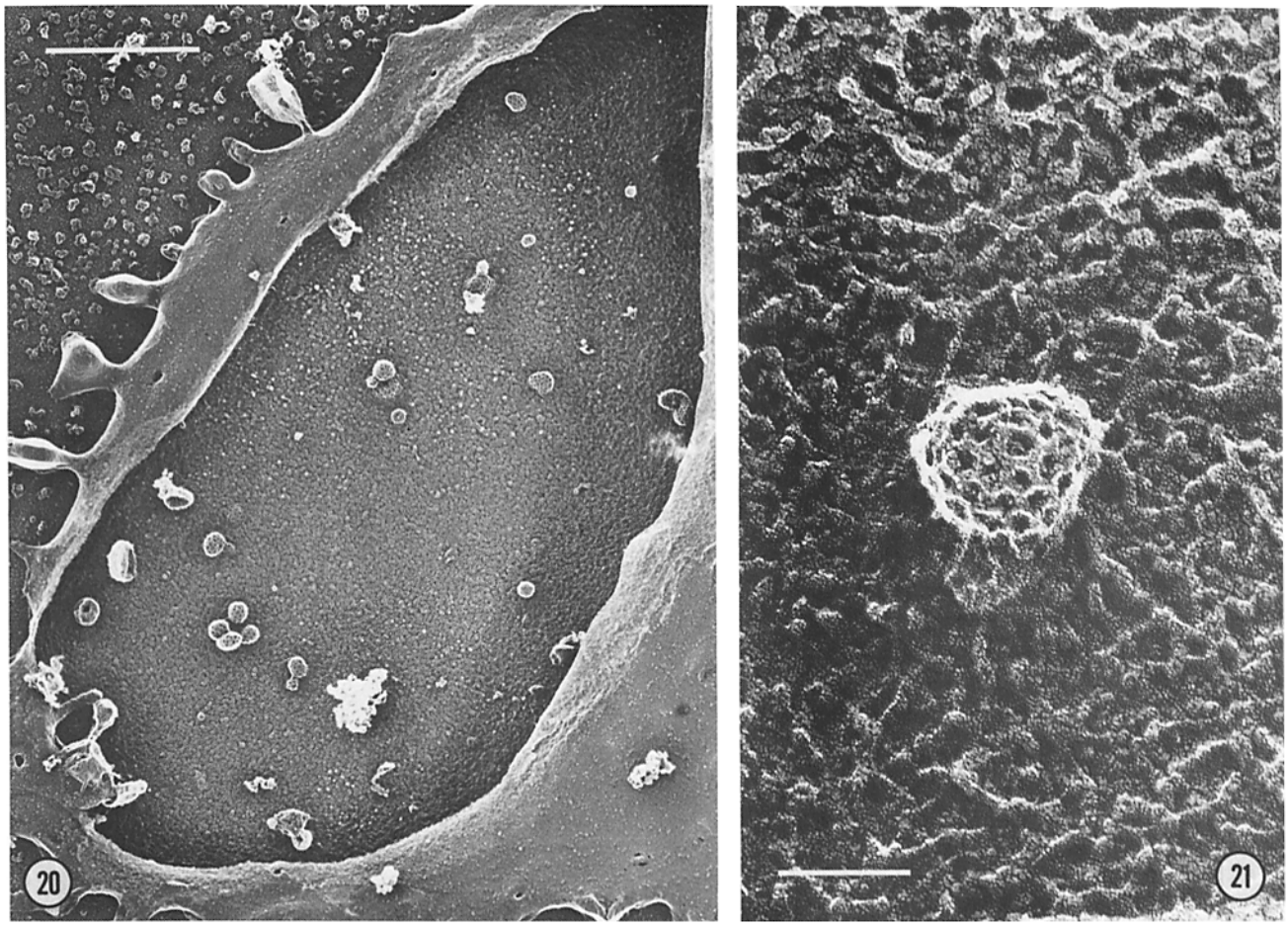

FIGURES 20 and 21 Fig. 20: View of the inside of a scraped-open reticulocyte, revealing the presence of numerous clathrin-coated domes. Bar, 500 nm. × 41,000. Fig. 21: Higher power view of a clathrin-coated dome surrounded by the anastomosing spectrin network of the reticulocyte cytoskeleton. Bar, 100 nm. × 179,000.

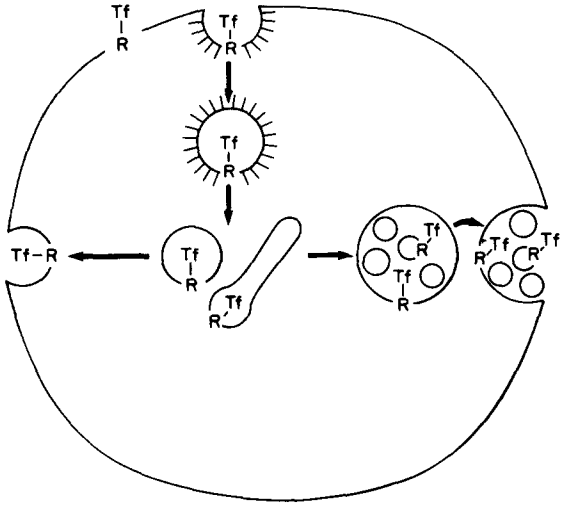

FIGURE 22 Possible routes of transferrin processing in reticulocytes. Transferrin is internalized via coated pits and vesicles. It rapidly appears inside small vesicles and tubules in the reticulocyte cytoplasm; subsequently it is transferred to MVE. Recycling appears to occur from MVE, but transferrin may also recycle directly from small vesicles or tubules to the cell surface.

with the released inclusions, indicating that transferrin receptors and possibly other membrane proteins may be extruded from the maturing reticulocyte by this form of exocytosis.

Fig. 22 illustrates the possible routes of transferrin and its receptor during processing by the reticulocyte. After transferrin binds to its receptor, it is internalized via coated pits and vesicles. Subsequently, it appears in small vesicles and tubular structures. Removal of iron from transferrin may occur inside these structures and/or inside MVE. Recycling to the plasma membrane may occur from the small vesicle or tubule compartment. Transferrin passes into MVE and may then also recycle to the plasma membrane.

We would like to thank Marilyn Levy for her invaluable assistance with the EM cytochemistry.

This work was supported by National Institutes of Health (NIH) grants GM 29647 and NS 17755 (J. Heuser); NIH grants GM 21096 and CA 12858 (P. Stahl); and Muscular Dystrophy Associations of America grants (J. Heuser and P. Stahl). C. Harding was supported by funds provided through an NIH Institutional Training Grant (GM 07200).

Received for publication 9 February 1983, and in revised form 29 April 1983.

REFERENCES

1. Bainton, D. F., and M. G. Farquhar. 1968. Differences in enzyme content of azurophil and specific granules of polymorphonuclear leukocytes. *J. Cell Biol.* 39:299–317.
2. Bentfeld-Barker, M. E., and D. F. Bainton. 1980. Cytochemical localization of arylsulfatase B in rat basophils and mast cells. *J. Histochem. Cytochem.* 28:1055–1061.
3. Come, S. E., S. B. Shohet, and S. H. Robinson. 1974. Surface remodeling vs. whole-cell hemolysis of reticulocytes produced with erythroid stimulation or iron deficiency anemia. *Blood.* 44:817–830.

4. Frazier, J. L., J. H.Caskey, M. Yoffe, and P. A. Seligman. 1982. Studies of the transferrin receptor on both human reticulocytes and nucleated human cells in culture. *J. Clin. Invest.* 69:853–865.
5. Galbraith, R. M., P. Werner, P. Arnaud, and G. M. P. Galbraith. 1980. Transferrin binding to peripheral blood lymphocytes activated by phytohemagglutinin involves a specific receptor. *J. Clin. Invest.* 66:1135–1143.
6. Glass, J., M. T. Nunez, and S. H. Robinson. 1977. Iron transport from Sepharose-bound transferrin. *Biochem. Biophys. Res. Commun.* 75:226–232.
6a. Harding, C., and P. Stahl. 1983. Transferrin recycling in reticulocytes: pH and iron are important determinants of ligand binding and processing. *Biochem. Biophys. Res. Commun.* 113:650–658.
7. Hemmaplardh, D., and E. H. Morgan. 1974. The mechanism of iron exchange between synthetic iron chelators and rabbit reticulocytes. *Biochim. Biophys. Acta.* 373:84–99.
8. Hemmaplardh, D., and E. H. Morgan. 1976. Transferrin uptake and release by reticulocytes treated with proteolytic enzymes and neuraminidase. *Biochim. Biophys. Acta.* 426:385–398.
9. Hemmaplardh, D., and E. H. Morgan. 1977. The role of endocytosis in transferrin uptake by reticulocytes and bone marrow cells. *Br. J. Haematol.* 36:85–96.
10. Heuser, J. 1981. Preparing biological samples for stereomicroscopy, by the quick-freeze, deep-etch, rotary-replication technique. *Methods Cell Biol.* 22:97–122.
11. Heuser, J., and L. Evans. 1980. Three-dimensional visualization of coated vesicle formation in fibroblasts. *J. Cell Biol.* 84:560–583.
12. Heuser, J. E., T. S. Reese, M. J. Dennis, Y. Jan, L. Jan, and L. Evans. 1979. Synaptic vesicle exocytosis captured by quick freezing and correlated with quantal transmitter release. *J. Cell Biol.* 81:275–300.
13. Hirokawa, N., and J. Heuser. 1982. The inside and outside of gap-junction membranes visualized by deep etching. *Cell.* 30:395–406.
14. Hirokawa, N., and J. E. Heuser. 1982. Internal and external differentiations of the postsynaptic membrane at the neuromuscular junction. *J. Neurocytol.* 11:487–510.
15. Horisberger, M. 1979. Evaluation of colloidal gold as a cytochemical marker for transmission and scanning electron microscopy. *Biol. Cell.* 36:253–258.
16. Hubbard, A. L., and H. Stukenbrok. 1979. An electron microscope autoradiographic study of the carbohydrate recognition systems in rat liver. II. Intracellular fates of ^{125}I-ligands. *J. Cell Biol.* 83:65–81.
17. Karin, M., and B. Mintz. 1981. Receptor-mediated endocytosis of transferrin in developmentally totipotent mouse teratocarcinoma cells. *J. Biol. Chem.* 256:3245–3252.
18. Kornfeld, S. 1968. The effects of structural modifications on the biologic activity of human transferrin. *Biochemistry.* 7:945–954.
19. Loh, T. T., Y. G. Yeung, and D. Yeung. 1977. Transferrin and iron uptake by rabbit reticulocytes. *Biochim. Biophys. Acta.* 471:118–124.
20. Morgan, E. H. 1981. Inhibition of reticulocyte iron uptake by NH_4Cl and CH_3NH_2. *Biochim. Biophys. Acta.* 642:119–134.
21. Morgan, E. H., and T. C. Appleton. 1969. Autoradiographic localization of ^{125}I-labelled transferrin in rabbit reticulocytes. *Nature (Lond.).* 223:1371–1372.
22. Morgan, E. H., G. Marsaglia, E. R. Giblett, and C. A. Finch. 1967. A method of investigating internal iron exchange utilizing two types of transferrin. *J. Lab. Clin. Med.* 69:370–381.
23. Nunez, M. T., J. Glass, S. Fischer, L. M. Lavidor, E. M. Lenk, and S. H. Robinson. 1977. Transferrin receptors in developing murine erythroid cells. *Br. J. Haematol.* 36:519–526.
24. Octave, J.-N., Y.-J. Schneider, R. R. Crichton, and A. Trouet. 1981. Transferrin uptake by cultured rat embryo fibroblasts: the influence of temperature and incubation time, subcellular distribution and short-term kinetic studies. *Eur. J. Biochem.* 115:611–618.
25. Octave, J.-N., Y.-J. Schneider, R. R. Crichton, and A. Trouet. 1982. Transferrin protein and iron uptake by isolated rat fibroblasts. *FEBS (Fed. Eur. Biochem. Soc.) Lett.* 137:119–123.
26. Octave, J.-N., Y.-J. Schneider, P. Hoffman, A. Trouet, and R. R. Crichton. 1982. Transferrin uptake by cultured rat embryo fibroblasts. The influence of lysosomotropic agents, iron chelators, and colchicine on the uptake of iron and transferrin. *Eur. J. Biochem.* 123:235–240.
27. Parmley, R. T., F. Ostroy, R. A. Gams, and L. DeLucas. 1979. Ferrocyanide staining of transferrin and ferritin-conjugated antibody to transferrin. *J. Histochem. Cytochem.* 27:681–685.
28. Shattil, S. J., and R. A. Cooper. 1972. Maturation of macroreticulocyte membranes in vivo. *J. Lab. Clin. Med.* 79:215–227.
29. Slot, J. W., and H. J. Geuze. 1981. Sizing of protein A-colloidal gold probes for immunoelectron microscopy. *J. Cell Biol.* 90:533–536.
30. Stahl, P., P. H. Schlesinger, E. Sigardson, J. S. Rodman, and Y. C. Lee. 1980. Receptor-mediated pinocytosis of mannose glycoconjugates by macrophages: characterization and evidence for receptor recycling. *Cell.* 19:207–215.
31. Sullivan, A. L., J. A. Grasso, and L. R. Weintraub. 1976. Micropinocytosis of transferrin by developing red cells: an electron-microscopic study utilizing ferritin-conjugated transferrin and ferritin-conjugated antibodies to transferrin. *Blood.* 47:133–143.
32. Tietze, C., P. Schlesinger, and P. Stahl. 1980. Chloroquine and ammonium ion inhibit receptor-mediated endocytosis of mannose-glycoconjugates by macrophages: apparent inhibition of receptor recycling. *Biochem. Biophys. Res. Commun.* 93:1–8.
33. Tietze, C., P. Schlesinger, and P. Stahl. 1982. Mannose-specific endocytosis receptor of alveolar macrophages: demonstration of two functionally distinct intracellular pools of receptor and their roles in receptor recycling. *J. Cell Biol.* 92:417–424.
34. Van Bockxmeer, F. M., and E. H. Morgan. 1979. Transferrin receptors during rabbit reticulocyte maturation. *Biochim. Biophys. Acta.* 584:76–83.
35. Van Renswoude, J., K. R. Bridges. J. B. Harford, and R. D. Klausner. 1982. Receptor-mediated endocytosis of transferrin and the uptake of Fe in K562 cells: identification of a non-lysosomal acidic compartment. *Proc. Natl. Acad. Sci. USA.* 79:6186–6190.
36. Verhoef, N. J., and P. J. Noordeloos. 1977. Binding of transferrin and uptake of iron by rat erythroid cells in vitro. *Clin. Sci. Mol. Med.* 52:87–96.
37. Wall, D. A., G. Wilson, and A. L. Hubbard. 1980. The galactose-specific recognition system of mammalian liver: the route of ligand internalization in rat hepatocytes. *Cell.* 21:79–93.
38. Ward, J. H., J. P. Kushner, and J. Kaplan. 1982. Regulation of HeLa cell transferrin receptors. *J. Biol. Chem.* 257:10317–10323.
39. Woodworth, R. C., A. Brown-Mason, T. G. Christensen, D. P. Witt, and R. D. Comeau. 1982. An alternative model for the binding and release of differic transferrin by reticulocytes. *Biochemistry.* 21:4220–4225.
40. Zaman, Z., M.-J. Heynen, and R. L. Verwilghen. 1980. Studies on the mechanism of iron uptake by rat reticulocytes. *Biochim. Biophys. Acta.* 632:553–561.
41. Zeitlin, P. L., and A. L. Hubbard. 1982. Cell Surface distribution and intracellular fate of asialoglycoproteins: a morphological and biochemical study of isolated rat hepatocytes and monolayer cultures. *J. Cell Biol.* 92:634–647.
42. Zweig, S. E., K. T. Tokuyasu, and S. J. Singer. 1981. Membrane-associated changes during erythropoiesis. On the maturation of reticulocytes to erythrocytes. *J. Supramol. Struct. Cell. Biochem.* 17:163–181.